Study of rare decay with P326 experiment at CERN SPS

V. N. Bolotov [*]

Institute for Nuclear Research

INR RAS, prospekt 60-letiya Oktyabrya 7a, Moscow 117312, Russia

Abstract

Experiment for study of ultra rare decay $K^+ \to \pi\nu\overline{\nu}(BR \sim 10^{-10})$ proposed at CERN is regarded. Main attention is devoted to the physical motivation and the cinematic to collect 80 events of this decay with ratio signal to background of 10:1. Here is given a short description of experimental setup.

Much attention has been attracted in INR for studying rare decays of elementary particles. Now our laboratory continuous data handling of experimental materials written on ISTRA setup. The performing of new OKA setup is also going on. At CERN it is planned a very powerful setup for studying rare decays with branching ratio up to 10^{-12} level. Many Russian groups would like to take part in this experiment. Our laboratory is working under performing detectors and programs for this experiment. The aim of these remarks is to attract attention to possibilities of this experiment. This work based on the Proposal published by big team from many physical centuries of different countries: CERN, Dubna, Ferrara, Florence, Frascati, Mainz, Mercsd, Moscow, Naples, Perugia, Protvino, Pisa, Rome, Saclay, Sofia, Turin [1].

The main goal of the experiment P326 (CERN) is to observe a sample of 80 $K^+ \to \pi\nu\nu$ events with small background. It permits to get value of CKM element $|V_{td}|$, constrain $\rho - \eta$ plane and Precisely to measure other kaon decays with larger but also small branching ratio.

Along with $B \to J/\Psi - K, B_s/B_d$ mixing and $K_L \to \pi^0\nu\nu$, the decay $K^+ \to \pi\nu\nu$ is one of the four "golden" modes that plays a critical role in over constraining the Standard Model description of CP violation. The leading contributions to this process are short-distance contribution (see.Fig.1, 2).

The branching ratio $K^+ \to \pi\nu\nu$ and $K^+ \to \pi^0 e^+\nu$ allows for extraction of $|V_{ts}{}^*V_{td}{}^*|$ [2],[3].

$$\frac{Br(K^+ \to \pi^+\nu\overline{\nu})}{Br(K^+ \to \pi^0 e^+\nu)} = \frac{3\alpha^2 r_+}{2\pi^2 \sin^4\theta_W |V_{us}|^2} \times |V_{cs}^* V_{cd} F(\frac{m_c}{m_W}) + V_{ts}^* V_{td} F(\frac{m_t}{m_W})|^2 \qquad (1)$$

In terms of the Wolfenstein parameterization:

$$\frac{Br(K^+ \to \pi^+\nu\overline{\nu})}{Br(K^+ \to \pi^0 e^+\nu)} = \frac{3\alpha^2 r_+}{2\pi^2 \sin^4\theta_W |V_{us}|^2} \times A^4\lambda^8 F^2(\frac{m_t}{m_W}) \times \frac{1}{\sigma}[(\rho_0 - \overline{\rho})^2 + (\sigma\overline{\eta})^2] \qquad (2)$$

where $r_+ = 0901$ corrects for phase space and isospin-breaking [4], $\sigma = 1/(1-\lambda^2/2)^2 = 1.050$, and $\rho_0 = 1 + \Delta$. $\Delta = 0.42 \pm 0.06$, and is the charm quark contribution.

This is the matrix V_{CKM} in the Wolfenstein parameterization as an expansion in powers $\lambda \equiv V_{us} = 0.2196 \pm 0.0023. A \equiv V_{cb}/\lambda 2$. To improve matrix to accuracy not worse $O(\lambda 6)$ the modified parameters are introduced:
$\overline{\rho} = \rho(1 - \lambda 2/2), \overline{\eta} = \eta(1 - \lambda 2/2)$.
The complex quantities $\lambda c = V_{cs}{}^*V_{cd}, \lambda_t = V_{ts}V_{td}$ have forms:

---

[*]**e-mail**: bolotovvn@mail.ru,bolotov@inr.ru
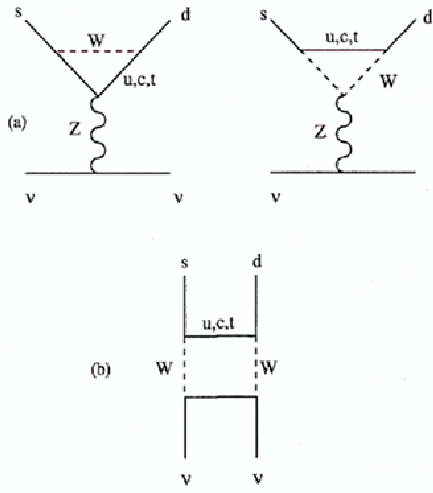
Figure 1: Diagrams for FCNC $s \to d\nu\bar{\nu}$ decays ($K \to \pi\nu\bar{\nu}$ decays): a)penguin diagrams, b) box diagram.
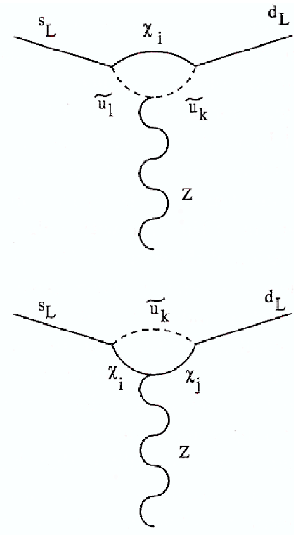
Figure 2: Diagrams containing SUSY contributions to the $Zd\bar{s}$ vertex.

On Fig.3 is shown well known CKM in the Wolfenstein parameterization.

$$
\mathbf{V_{CKM}} = \begin{pmatrix} 1 - \frac{\lambda^2}{2} & \lambda & A\lambda^3(\varrho - i\eta) \\ -\lambda & 1 - \frac{\lambda^2}{2} & A\lambda^2 \\ A\lambda^3(1 - \varrho - i\eta) & -A\lambda^2 & 1 \end{pmatrix} + O(\lambda^4).
$$
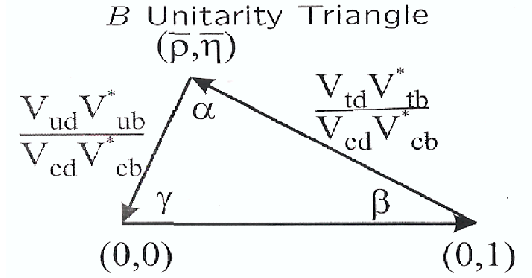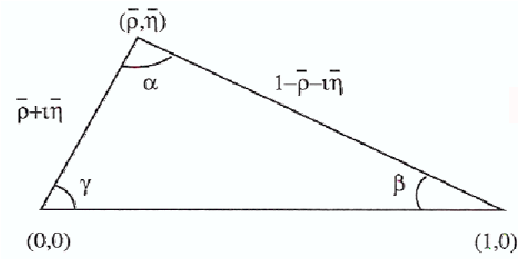
Figure 3: Graphical representations in the ρ and $i\eta$ plane of the unitary condition.

$$
\left.
\begin{array}{rcl}
Re\lambda_c & \simeq & -\lambda(1 - \frac{\lambda^2}{2}) + O(\lambda^5) \\
Im\lambda_c & \simeq & -\eta A^2\lambda^5 + O(\lambda^7) \\
Re\lambda_t & = & -A^2\lambda^5(1 - \frac{\lambda^2}{2})(1 - \underline{\rho}) + O(\lambda^7) \\
Im\lambda_t & = & \eta A^2\lambda^5 + O(\lambda^9)
\end{array}
\right\}
$$

Near 80 $K^+ \to \pi\nu\bar{\nu}$ events gives approximately 10% precision value $|V_{td}|$. Simultaneous measurement of two "gold" decays $K^+ \to \pi\nu\bar{\nu}$ and $K_L \to \pi^0\nu\nu$ is extremely important, because branching ratios of them both proportional to $|Vcb|$.

On Fig.3 presents unitary triangles in terms of Wolfenstein parameters and CKM elements. The V_{CKM} unitarily condition is $V_{ud}V_{ub}{}^* + V_{td}V_{tb}{}^* = -V_{cd}V_{cb}{}^*$ or in Wolf. par.:

$A_{\lambda3}(\bar{\rho} + i\bar{\eta}) + A_{\lambda3}(1 - (\bar{\rho} + i\bar{\eta})) = A_{\lambda3}$. After normalization by $A_{\lambda3}$ it may be presented

as a triangle in complex plane $(\bar{\rho}, \bar{\eta})$, as shown in Fig 3.

2

The widths of $K^+ \to \pi^+ \nu \bar{\nu}$ and well known $K^+ \to \pi^0 e^+ \nu$ decays are:

$$\Gamma(K^+ \to \pi^+ \nu \bar{\nu}) = \left(\frac{G_F}{\sqrt{2}}\right)^2 \cdot |(\pi^+ \nu \bar{\nu}|H_w|K^+)|^2 \cdot 3 \left(\frac{\alpha}{2\pi \sin^2 \vartheta_w}\right)^2 \cdot |\lambda_c F(x_c) + \lambda_t F(x_t)|^2 \quad (3)$$

$$\Gamma(K^+ \to \pi^0 e^+ \nu_e) = \left(\frac{G_F}{\sqrt{2}}\right)^2 \cdot |V_{us}|^2 \cdot |(\pi^0 e^+ \nu_e|H_w|K^+)|^2 \quad (4)$$

Relations between these processes and branching ratio of $K^+ \to \pi \nu \nu$ are given:

$$\left|\frac{(\pi^+ \nu \bar{\nu}|H_w|K^+)}{(\pi^0 e^+ \nu_e|H_w|K^+)}\right|^2 = \left|\frac{(\pi^+|H_w|K^+)}{(\pi^0|H_w|K^+)}\right|^2 = 2r_+ \quad (5)$$

This relation comes from isotopic-spin symmetry, $r_+ = 0.901$ from the phase space correction and the breaking of isotopic symmetry. Branching ratio for $K^+ \to \pi \nu \nu$ decay is

$$Br(K^+ \to \pi^+ \nu \bar{\nu}) = R_+ \cdot \frac{|\lambda_c F(x_c) + \lambda_t F(x_t)|^2}{|V_{us}|^2} \quad (6)$$

$$R_+ = \left[Br(K^+ \to \pi^0 e^+ \nu_e) \cdot \frac{3\alpha^2}{2\pi^2 \sin^4 \vartheta_w} \cdot r_+\right] = 7.50 \times 10^{-6} \quad (7)$$

$$
\begin{aligned}
|\lambda_c F(x_c) + \lambda_t F(x_t)|^2 &= [Re\lambda_c \cdot F(x_c) + Re\lambda_t \cdot F(x_t)]^2 + [Im\lambda_c \cdot F(x_c) + Im\lambda_t \cdot F(x_t)]^2 \simeq \\
&\simeq [Re\lambda_c \cdot F(x_c) + Re\lambda_t \cdot F(x_t)]^2 + [Im\lambda_t \cdot F(x_t)]^2 \simeq \\
&\simeq [-\lambda^5 (1 - \frac{\lambda^2}{2})A^2 F(x_t)(\rho_0 - \bar{\rho})]^2 + [\lambda^5 (1 - \frac{\lambda^2}{2})A^2 F(x_t)\sigma \eta]^2 \simeq \\
&\simeq \lambda^{10} \cdot A^4 \cdot F(x_t)^2 \cdot \frac{1}{\sigma}[(\rho_0 - \bar{\rho})^2 + (\sigma \bar{\eta})^2]
\end{aligned}
\quad (8)
$$

Here the following notations have been introduced:

$$
\left.
\begin{aligned}
\rho_0 &= 1 + \Delta \\
\Delta &= F(x_c)/[A^2 \lambda^4 F(x_t)] = 0.42 \pm 0.06 \\
\sigma &= 1/(1 - \lambda^2/2)^2 = 1.050
\end{aligned}
\right\}
\quad (9)
$$

$$
\begin{aligned}
Br(K^+ \to \pi^+ \nu \bar{\nu})\Big|_{SM} &= R_+ A^4 \lambda^8 F(x_t)^2 \frac{1}{\sigma}[(\rho_0 - \bar{\rho})^2 + (\sigma \bar{\eta})^2] = \\
&= R_+ |V_{cb}|^4 F(x_t)^2 \frac{1}{\sigma}[(\rho_0 - \bar{\rho})^2 + (\sigma \bar{\eta})^2] = \\
&= (0.77 \pm 0.21) \cdot 10^{-10}
\end{aligned}
\quad (10)
$$

The parameters are taken from Table 1. The theoretical prediction for branching ratio for $K^+ \to \pi \nu \nu$ decay is mainly limited by the c-quark contribution and is to $\sim 5\%$. V_{td}, V_{ts} and V_{tb} are obtained not from direct t-decays, but from V_{CKM} unitarity conditions (see above). Values of the relevant parameters are used to obtain numerical estimates taken from different experimental and theoretical sources (Table 1).

$$
\begin{aligned}
\lambda = |V_{us}| &= 0.2196 \pm 0.0023 \\
\overline{\rho} &= 0.223 \pm 0.038 \\
\overline{\eta} &= 0.316 \pm 0.039 \\
|V_{cb}| &= (41.0 \pm 1.6) \cdot 10^{-3} \\
|V_{ub}| &= (35.5 \pm 3.6) \cdot 10^{-4} \\
A = V_{cb}/\lambda^2 &= 0.819 \pm 0.049 \\
\sin 2\beta &= 0.70 \pm 0.07 \\
m_t = \overline{m}_t &= 167 \pm 5 \text{ GeV} \\
F(x_t) &= 1.53 \pm 0.05 \\
\rho_0 = 1 + \tfrac{P_0}{A^2 \cdot F(x_t)} = 1 + F(x_c)/A^2\lambda^4 F(x_t) &= 1.42 \pm 0.06 \\
\xi = f_{B_s}\sqrt{B_s}/f_{B_d}\sqrt{B_d} &= 1.14 \pm 0.06 \\
m_{B_d^0} &= 5.2792 \text{ GeV} \\
m_{B_s^0} &= 5.3693 \text{ GeV} \\
m_\omega &= 80.41 \text{ GeV}
\end{aligned}
$$

Figure 4 is an idealized diagram showing the connection between the position of the apex of this triangle and various physical processes.
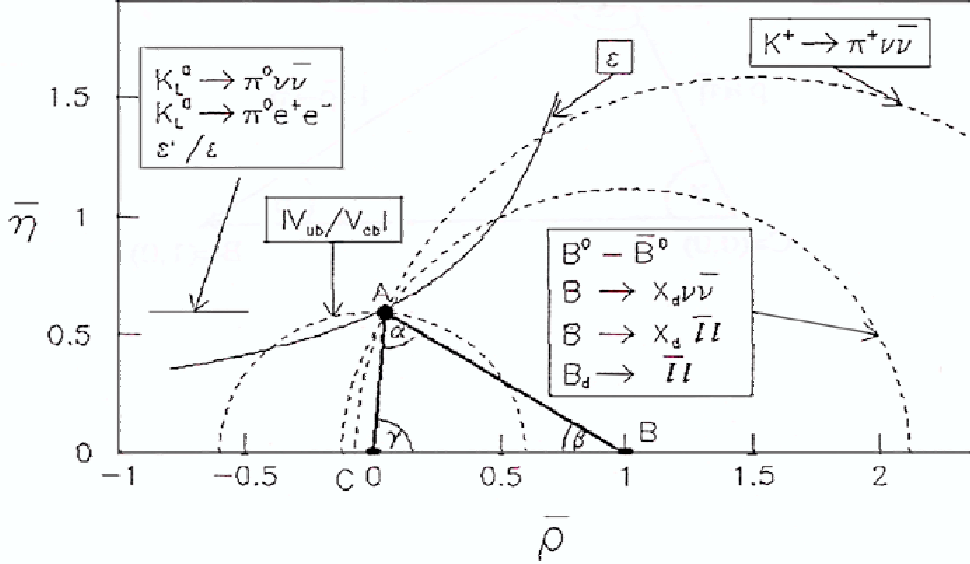
Figure 4: The ideal unitary triangle.

In reality, the current theoretical and experimental uncertainties constrained in ρ, η lie in the regions as shown in Fig. 5.
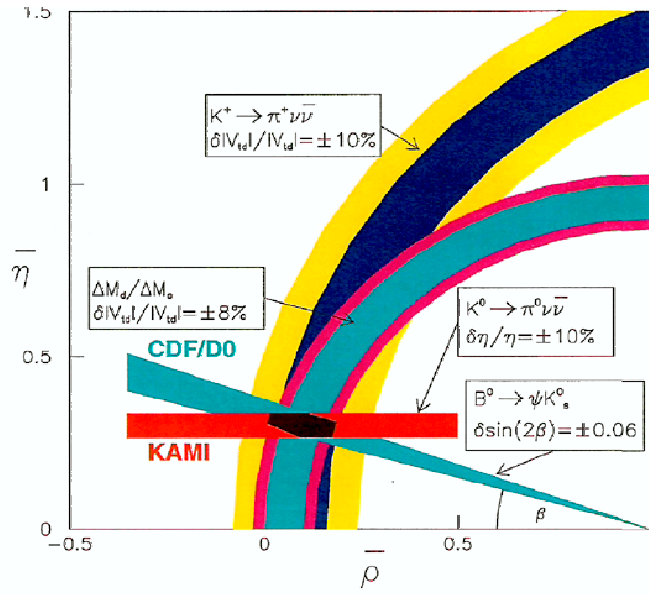
Figure 5: A possible outcome for $\overline{\rho}, \overline{\eta}$ and β obtained from future K-meson experiments:

$K^+ \rightarrow \pi^+ \nu\overline{\nu}(P326); K_L{}^0 \rightarrow \pi^0 \nu\overline{\nu}$ (KAMI,/KOPIO) and $\Delta m B_d / \Delta m B_s; B^0(\overline{B}^0) \rightarrow J/\Psi K_S{}^0$. The light region includes possible theoretical uncertainties in $Br(K^+ \rightarrow \pi^+ \nu\nu))$ connected with the influence of C-quarks.

The experimental layout is shown in Fig. 6 .
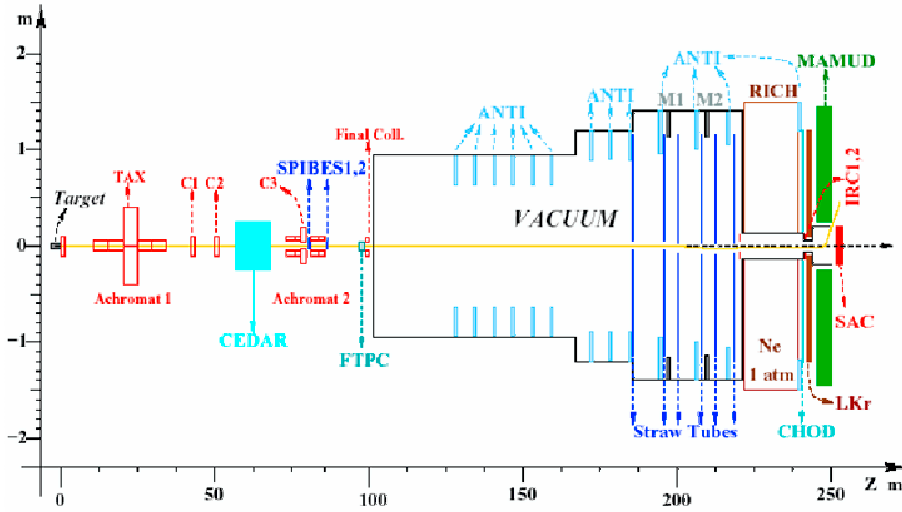
Figure 6: Detector layout.

1. CEDAR - a differential Cherenkov counter placed on the incoming beam to tag kaons.
2. GIGATRTRACKER.

SPIBES (FAST PIXEL) - thin silicon micro-pixel detector for momentum measurement of the incoming beam with sub-nanosecond time resolution to provide a tight time coincidence between the kaon and the pion tracks to simplify the pattern recognition in the gas TPC 12 m downstream.

FTPC (Micromegas-based Flash-TPC) - a gas Time Projection Chamber to measure of the incoming beam particles with the least amount of material to minimize the effect of multiple scattering.

5

3. ANTI - a set of ring-shaped anti-counters surrounding the vacuum tank and providing full coverage for photons originating from the decay region with the angles as large as 50 mr.

4. STRAW TRACKER - a double magnetic spectrometer measuring the direction of the out-going pion and its momentum. Chambers of straw tubes can operate in vacuum.

5. RICH - a gas Ring Imaging Cherencov counter providing muon/pion separation.

6. CHOD - a hodoscope for triggering and precise timing of charged track, based on multi-gap glass RPCs.

7. LKR - a high-performance electromagnetic calorimeter acting as photon veto in angular region 1.0and 15.0 mr.

8. MAMUD - a magnetized hadron calorimeter and muon detector capable of identifying muons with inefficiencies smaller than 10-5. It also serves to deflect the beam away from the photon detector (SAC).

9. IRC1-2,SAC - intermediate ring and small angle photon veto calorimeters covering the angular regions around and in beam.

In Table 2 the most frequent kaon decays are presented with the techniques intended to reject them. The kinematics of some these decays are compared to the investigated decay are shown in Fig.7.

Table 2:

Dekay Mode	Branching Ratio	Background Rejection
$K^+ \rightarrow \mu^+\nu$	63% (called $K_{\mu 2}$)	μ PID, Two-Body Kinematics
$K^+ \rightarrow \pi^+\pi^0$	21%	Photon Veto, Two-Body Kinematics
$K^+ \rightarrow \pi^+\pi^+\pi^-$	6%	Charged Particle Veto,Kinematics
$K^+ \rightarrow \pi^+\pi^0\pi^0$	2%	Photon Veto, Kinematics
$K^+ \rightarrow \pi^0\mu^+\nu$	3% (called $K_{\mu 3}{}^+$)	Proton Veto, μ PID
$K^+ \rightarrow \pi^0 e^+\nu$	5% (called $K_{e3}{}^+$)	Photon Veto, E/ρ

To separate the $K^+ \rightarrow \pi^+\nu\overline{\nu}$ decay from main background decays is convenient to use squared missing mass variable $m_{miss}{}^2$ (see Fig. 8).
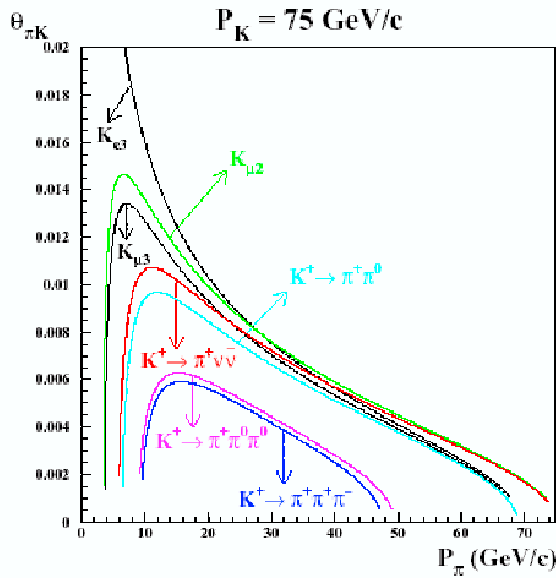
Figure 7: Fig.7. A comparison of the charged track angle-momentum relation for the most frequents K+ decays and $K^+ \rightarrow \pi^+\nu\overline{\nu}$. For the three-body decays, the curves indicate the kinematical limit.

The two undetectable neutrinos in the final state require the design of the experiment with redundant measurement of the event kinematics and hermetic veto's to achieve a background rejection $S/B \sim 10$. The main background source comes from the decays $K^+ \rightarrow \pi^+\pi^0$ and well $K^+ \rightarrow \mu^+\nu$. To reduce the background it is planned to use kinematics cut on missing mass.

$$m^2_{miss} \simeq m^2_K \left(1 - \frac{|P_\pi|}{|P_K|}\right) + m^2_\pi \left(1 - \frac{|P_K|}{|P_\pi|}\right) - |P_K||P_\pi|\theta^2_{\pi K} \tag{11}$$

Without resolution effects, the m^2_{miss} distribution for $K^+ \rightarrow \pi^+\pi^0$ is line at $m^2_{miss} = m^2_{\pi 0}$. The distribution for $K^+ \rightarrow \pi^+\nu\overline{\nu}$ overlaps this line and can be divided into two regions

(I) $0 < m^2_{miss} < m^2_{\pi 0} - (\Delta m)^2$

(II) $m^2_{\pi 0} + (\Delta m)^2 < min(m^2_{miss}(\pi^+\pi^+\pi^-)) - (\Delta m)^2$,where Δm term depends on the resolution. See Fig.8.
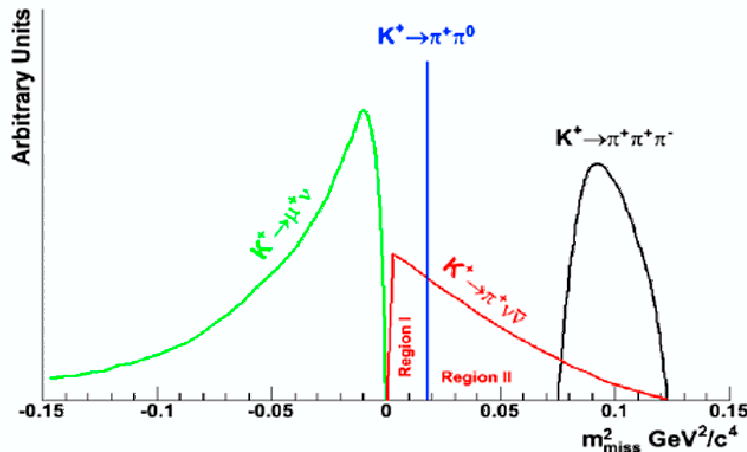
Figure 8: Distribution of the missing mass squared for the signal and most frequent kaon decays

Assuming the veto inefficiency on π^0 to be 10^{-8} and the muon veto inefficiency at the level of 5×10^{-6} , Simulations have shown that $S/B \geq 10$ with signal acceptance larger than 10% can be achieved with $(\Delta m)^2 \sim 8 \times 10^{-3} GeV^2/c^4$. With a resolution on kaon momentum 0.3% , a resolution of the pion momentum 1% at 30 GeV/c and a resolution $\theta_{\pi k}$ of 50 μrad, it is able to achieve the m^2_{miss} resolution in order to reject cinematically the backgrounds at the required level.

References

[1] Proposal to Measure the Rare Decay $K^+ \rightarrow \pi^+\nu\nu$
   at the CERN SPS. Preprint CERN-SPSC-P-326-013, SPSC-P-326, 116.2005.

[2] T. Inami, C.S. Lim, Prog. Theor. Phys. 65, 297(1981).

[3] G Buchalla, Z. Buras, Phys. Rev. D54,6782 (1996).

[4] W. Marciano, Z. Parsa, Phys. Rev. D53, R1 (1996).